

Performance of Spatially-Coupled LDPC Codes and Threshold Saturation over BICM Channels

Arvind Yedla, *Member, IEEE*, Mostafa El-Khamy, *Senior Member, IEEE*, Jungwon Lee, *Senior Member, IEEE*, and Inyup Kang, *Member, IEEE*

Abstract—We study the performance of binary spatially-coupled low-density parity-check codes (SC-LDPC) when used with bit-interleaved coded-modulation (BICM) schemes. This paper considers the cases when transmission takes place over additive white Gaussian noise (AWGN) channels and Rayleigh fast-fading channels. The technique of upper bounding the maximum-a-posteriori (MAP) decoding performance of LDPC codes using an area theorem is extended for BICM schemes. The upper bound is computed for both the optimal MAP demapper and the suboptimal max-log-MAP (MLM) demapper. It is observed that this bound approaches the noise threshold of BICM channels for regular LDPC codes with large degrees. The rest of the paper extends these techniques to SC-LDPC codes and the phenomenon of threshold saturation is demonstrated numerically. Based on numerical evidence, we conjecture that the belief-propagation (BP) decoding threshold of SC-LDPC codes approaches the MAP decoding threshold of the underlying LDPC ensemble on BICM channels. Numerical results also show that SC-LDPC codes approach the BICM capacity over different channels and modulation schemes.

Index Terms—BICM, Rayleigh fast-fading, density evolution, GEXIT curves, LDPC codes.

I. INTRODUCTION

The phenomenon of threshold saturation was introduced by Kudekar et al. [1] to explain the impressive performance of convolutional low-density parity-check (LDPC) ensembles [2], [3]. These codes are essentially terminated convolutional codes with large memory, which admit a sparse parity-check matrix representation. One way to construct these codes is to “spatially-couple” an underlying LDPC ensemble, resulting in a spatially-coupled LDPC (SC-LDPC) ensemble. It was observed that the belief-propagation (BP) threshold of a spatially-coupled ensemble is very close to the maximum-a-posteriori (MAP) threshold of its underlying ensemble; a similar statement was formulated independently, as a conjecture in [4]. This phenomenon has since been called “threshold saturation via spatial coupling”. Kudekar et al. prove in [1] that threshold saturation occurs for the binary erasure channel (BEC) and a particular class of underlying regular LDPC ensembles. For general binary-input memoryless symmetric (BMS) channels, threshold saturation was empirically observed first [5], [6] and then analytically shown [7], [8]. It is known that the MAP threshold of regular LDPC codes approaches the Shannon limit for binary memoryless symmetric (BMS) channels with increasing left degree, while keeping the rate fixed (though such codes have a vanishing BP threshold) [1]. So, spatial coupling provides us with a technique to construct a single capacity approaching code ensemble for all BMS channels

with a given capacity. This technique is indeed very general and has since been applied to a broad class of graphical models. A good summary of recent applications of spatial coupling can be found in [8].

In this paper, we evaluate the performance of spatially-coupled LDPC codes using BICM schemes for transmission over additive white Gaussian noise (AWGN) and Rayleigh fast-fading channels. The noise threshold, a.k.a. the Shannon limit, for bit-interleaved coded-modulation (BICM) schemes can be computed using Monte-Carlo simulations via the generalized mutual information (GMI) [9]. This method can be used to compute the information theoretic limits for different suboptimal BICM schemes and is briefly reviewed in Section II-B. We review density evolution (DE) for BICM schemes, described in [10, Sec. 5.2], in Section II-C. We note that the above DE can be greatly simplified by using the Gaussian mixture approximation for the BICM bit-channels presented in [11], to obtain approximate thresholds. Section III extends the GEXIT analysis and the upper bounding technique on the MAP decoding threshold for BICM schemes. Section IV extends the analysis to SC-LDPC codes. The DE results of SC-LDPC codes are presented in Section V and some concluding remarks are given in Section VI.

II. BACKGROUND

A. The BICM Model

BICM is a practical approach to coded modulation and was introduced by Zehavi in [12]. A comprehensive analysis for BICM is provided in [10], which is an excellent reference for BICM. We now briefly describe the BICM model and the problem setup. Consider transmission over a memory-less channel with input alphabet \mathcal{X} (with $|\mathcal{X}| = 2^M$, $M \in \mathbb{N}$) and output alphabet \mathbb{C} . We use uppercase letters (e.g., X, Y) to denote random variables and lowercase letters (e.g., x, y) to denote their corresponding realizations. The channel output is given by

$$Y = AX + Z, \quad (1)$$

where $X \in \mathcal{X}$, $Y \in \mathbb{C}$, and Z is additive Gaussian noise with variance σ^2 i.e., $Z \sim \mathcal{CN}(0, \sigma^2)$. We consider the cases of no fading ($A = 1$) and Rayleigh fast-fading ($A \sim \mathcal{CN}(0, 1)$). Furthermore, we assume that the receiver has perfect channel state information for simplicity. The analysis can be easily extended to the case when the receiver does not have access to the channel state information [13], [14, Sec. 5.1].

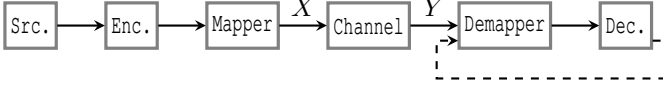


Fig. 1. The BICM system model. The codeword is mapped to a symbol $X \in \mathcal{X}$ using the mapper. The channel output Y is then passed through a demapper which performs the symbol-to-bit metric calculation. The decoder output can be optionally fed back to the demapper as apriori information for BICM-ID.

A Bernoulli-(1/2) source is encoded using an LDPC code chosen uniformly at random from the standard irregular ensemble LDPC(N, λ, ρ) [14, Ch. 3]. Here, $\lambda(x) = \sum_i \lambda_i x^{i-1}$ is the degree distribution (from an edge perspective) corresponding to the variable nodes and $\rho(x) = \sum_i \rho_i x^{i-1}$ is the degree distribution (from an edge perspective) of the parity-check nodes in the decoding graph.¹ The coefficient λ_i (resp. ρ_i) gives the fraction of edges that connect to variable nodes (resp. parity-check nodes) of degree i . Likewise, let L_i be the fraction of variable nodes with degree i and define $L(x) = \sum_i L_i x^i$. The design rate of the LDPC code is given by

$$R(\lambda, \rho) = 1 - \frac{\int_0^1 \rho(x) dx}{\int_0^1 \lambda(x) dx}.$$

The blocklength N is assumed to be a multiple of M , where groups of M bits are mapped to a symbol in \mathcal{X} and then transmitted over the channel. At the receiver, a demapper first performs the symbol-to-bit metric calculation based on the received symbol Y , and the metrics are then passed to the decoder. One can also perform the symbol-to-bit metric calculation iteratively, by using the decoder output as apriori information at the demapper. This scheme is commonly known in the literature as BICM iterative detection (BICM-ID). The block diagram of a general BICM system is shown in Fig. 1.

A BICM scheme is specified by the bit-to-symbol mapper and the demapper. Throughout this work, we consider square quadrature amplitude modulation (QAM) constellations with the Gray mapping scheme, and the optimal MAP and suboptimal max-log-MAP (MLM) demappers.

B. Noise Threshold of BICM Channels

Consider the case when the demapper calculation is not updated between iterations. The performance of the BICM scheme (for optimal demappers) is given by the capacity of a set of parallel independent channels [15]. It was also characterized in terms of the generalized mutual information (GMI) by viewing the BICM decoder as a mismatched decoder [16]. The GMI analysis was used in [17] to compute the performance of BICM in the presence of suboptimal demappers. The achievable information rate of a given BICM scheme can be computed using Monte-Carlo simulations via the GMI [9]. Consider a BICM channel with M -bits per symbol. The I -curve was introduced in [9] and can be computed for the m -th

¹The edges of the variable nodes connected to the demapper are not included in the degree profile.

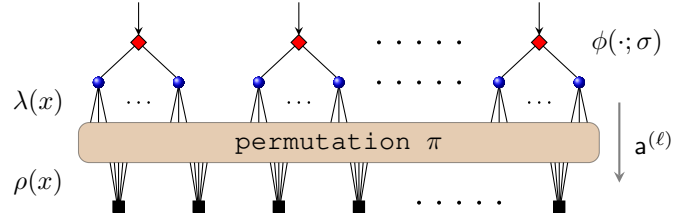


Fig. 2. The Tanner graph at the decoder for BICM channels. The red diamonds represent the demapper nodes, the blue circles and black squares represent the variable and check nodes respectively. Each demapper node is connected to M variable nodes.

bit level via

$$I_m(s; \sigma) = 1 - \mathbb{E}_{X, Y} \log(1 + \exp((2b_m(X) - 1)\Lambda_m(Y(\sigma))s)),$$

where X and Y are the channel input and output respectively (we have used the notation $Y(\sigma)$ to make explicit the dependence on the channel noise variance), $b_m(X)$ is the m -th bit label of symbol X and $\Lambda_m(Y)$ is the log-likelihood ratio of the m -th bit of the symbol after passing through the demapper [9]. The I -curve of the BICM channel is then computed as

$$I(s; \sigma) = \sum_{m=0}^{M-1} I_m(s; \sigma).$$

The achievable information rate of the BICM scheme is equal to the GMI, given by $I(\sigma) = \max_s I(s; \sigma)$. This enables us to compute the achievable information rate of BICM schemes, for different modulation schemes, bit-to-symbol mappings and demappers. The noise threshold for error-free transmission at a given transmission rate R can then be computed for a specific BICM scheme by $\sigma^* = I^{-1}(R)$.

For the case of BICM-ID, the capacity would be equal to the coded modulation capacity, when the input alphabet is restricted to \mathcal{X} . The noise threshold can be computed for this case similarly. Let $I(\sigma) = I(X; Y(\sigma))$, when the input is uniformly distributed. Then the noise threshold for BICM-ID is given by $\sigma^* = I^{-1}(R)$.

C. Density Evolution

We begin this section by first introducing some notation. Let v_i , c_j and d_k denote the variable, check and demapper nodes respectively. Let $\pi(k, m) \triangleq (k-1)M + m = i$, be the mapping from the demapper nodes to the variable nodes i.e., the m -th bit of demapper node k is connected to variable node i . When the symbol index k is understood from context, we write $\pi(m) = i$, and $m = \pi^{-1}(i)$. The m -th bit corresponding to $x \in \mathcal{X}$ is denoted by $b_m(x)$, and the set of symbols where the m -th bit is zero (one) is denoted by \mathcal{X}_0^m (\mathcal{X}_1^m).

The factor graph structure at the joint decoder is shown in Fig. 2. The joint decoder proceeds by performing one round of decoding for the LDPC code followed by a demapper update. This is the schedule for BICM-ID. To reduce the complexity non-iterative detection is used, where the demapper update is not performed between iterations.

Let $\mu_{v_i \rightarrow c_j}^{(\ell)}$, $\mu_{c_j \rightarrow v_i}^{(\ell)}$, $\mu_{v_i \rightarrow d_k}^{(\ell)}$ and $\mu_{d_k \rightarrow v_i}^{(\ell)}$ be the messages from the bit node to check node, check node to variable node, variable node to demapper node and demapper node to variable

node during iteration ℓ respectively. All the messages are in log-likelihood ratio domain. The message passing rules at the variable and check nodes are the standard rules and their description is omitted. Using the notation ∂i to denote the set of check nodes connected to variable node i , the message $\mu_{v_i \rightarrow d_k}^{(\ell)}$ is given by

$$\mu_{v_i \rightarrow d_k}^{(\ell)} = \sum_{j \in \partial i} \mu_{c_j \rightarrow v_i}^{(\ell)}.$$

Let m be the bit index corresponding to variable node v_i i.e., $m = \pi^{-1}(i)$ and B_m be the random variable corresponding to that bit. The bit probabilities in the ℓ -th iteration can be computed using the variable node to demapper node messages via

$$\Pr(B_m=0) = \frac{e^{\mu_{v_i \rightarrow d_k}^{(\ell)}}}{1 + e^{\mu_{v_i \rightarrow d_k}^{(\ell)}}}, \Pr(B_m=1) = \frac{1}{1 + e^{\mu_{v_i \rightarrow d_k}^{(\ell)}}}.$$

So, the demapper to variable node message is given by

$$\mu_{d_k \rightarrow v_i}^{(\ell)} = \log \frac{\sum_{x \in \mathcal{X}_0^m} p(y_k|x) \prod_{l \neq m} \Pr(B_{\pi(l)} = b_{\pi(l)}(x))}{\sum_{x \in \mathcal{X}_1^m} p(y_k|x) \prod_{l \neq m} \Pr(B_{\pi(l)} = b_{\pi(l)}(x))}, \quad (2)$$

where $B_{\pi(l)}$ is used to denote the bit corresponding to variable node $v_{\pi(k,l)}$ and is an abuse of notation. The above message passing rule is for the optimal MAP demapper. The rule for the MLM demapper is obtained by performing the standard approximation of the above equation to reduce complexity. The variable nodes $i = 1, \dots, N$ can be grouped into equivalence classes via the function $\pi(k, m)$ i.e., let $V_m = \{v_i | \pi(k, m) = i, k = 1, \dots, N/M\}$ denote the set of all variable nodes connected to the m -th bit of the demapper nodes. Denote the density of messages emanating from the variable nodes in V_m to the check nodes at iteration ℓ by $\mathbf{a}_m^{(\ell)}$, conditioned on the transmission of an all-zero codeword. Note that the all-zero codeword assumption is not valid, but we can still use DE with standard symmetrizing techniques [14], [18, Ch. 7]. The transformation of the densities of the incoming messages at the check node and variable node are denoted by \boxtimes and \otimes respectively (see discussion in [14, p. 181]). For a density \mathbf{x} , we denote

$$\mathbf{x}^{\boxtimes n} \triangleq \underbrace{\mathbf{x} \boxtimes \mathbf{x} \boxtimes \dots \boxtimes \mathbf{x}}_n,$$

and likewise for $\mathbf{x}^{\otimes n}$. Using this notation, define $\lambda(\mathbf{x}) = \sum_i \lambda_i \mathbf{x}^{\otimes(i-1)}$, $\rho(\mathbf{x}) = \sum_i \rho_i \mathbf{x}^{\boxtimes(i-1)}$ and $L(\mathbf{x}) = \sum_i L_i \mathbf{x}^i$.

The density of messages at the input to the check nodes is given by

$$\mathbf{a}^{(\ell)} = \frac{1}{M} \sum_{m=1}^M \mathbf{a}_m^{(\ell)}. \quad (3)$$

We call $\mathbf{a}^{(\ell)}$ the average density of messages from the variable node to check node at iteration ℓ . The density of messages from the variable node to the demapper node is then given by $L(\rho(\mathbf{a}^{(\ell)}))$. Let $\phi_m(\cdot; \sigma)$ be the demapper density transformation operator of the m -th bit corresponding to (2). Then, the

density evolution equations are given by

$$\begin{aligned} \mathbf{a}_m^{(\ell+1)} &= \phi_m \left(L(\rho(\mathbf{a}^{(\ell)})); \sigma \right) \otimes \lambda \left(\rho(\mathbf{a}^{(\ell)}) \right) \\ \mathbf{a}^{(\ell)} &= \frac{1}{M} \sum_{m=1}^M \mathbf{a}_m^{(\ell)}, \end{aligned} \quad (4)$$

from which one obtains the recursion

$$\mathbf{a}^{(\ell+1)} = \phi \left(L(\rho(\mathbf{a}^{(\ell)})); \sigma \right) \otimes \lambda \left(\rho(\mathbf{a}^{(\ell)}) \right),$$

where $\phi(\cdot; \sigma)$ maps the incoming density at the demapper node to the average output density i.e.,

$$\phi(\mathbf{x}; \sigma) = \frac{1}{M} \sum_{m=1}^M \phi_m(\mathbf{x}; \sigma).$$

One can use the ‘ M ’ equations (4) to perform DE for protograph based LDPC codes to design bit mappings for optimal performance, similar to [19] where the authors use PEXIT curves for optimization. This function does not have a closed form expression and can be computed using Monte-Carlo simulations.

III. GEXIT CURVES FOR BICM

In this section, we derive an expression for the BP-GEXIT curve for LDPC codes for BICM schemes. Using the BP-GEXIT curve and the area theorem, an upper bound is derived for the MAP decoding threshold of LDPC codes for BICM schemes. As defined in the previous section, let $\pi(k, m) = (k-1)M + m = i$, be the mapping from the demapper nodes to the variable nodes. In this section, boldface uppercase letters (e.g. \mathbf{X}, \mathbf{Y}) are used to denote random vectors and $\mathbf{X}_{\sim k}$ to denote the vector with all elements of \mathbf{X} except the k -th element. Let $x_k^{[m]}$ be the m -th bit of symbol k and let $i = \pi(k, m)$. Throughout this section, variable node v_i shall be denoted by $x_k^{[m]}$ via the function π . Consider transmission over the BICM channel family (1) parametrized by the normalized channel entropy per bit, given by

$$\alpha = \frac{1}{M} H(\mathbf{X}|\mathbf{Y}).$$

We note that $\alpha \in [0, 1]$ and that the channel family is complete and degraded with respect to α . Let $\mathbf{X} \in \mathcal{X}^{N/M}$ be the transmitted vector and \mathbf{Y} be the output of the channel. Following the definition for BMS channels [14, Ch. 4], the GEXIT function for BICM channels is defined as

$$\mathbf{g}(\alpha) = \frac{1}{N} \frac{dH(\mathbf{X}|\mathbf{Y}(\alpha))}{d\alpha},$$

and satisfies an area theorem by definition:

$$\begin{aligned} \int_0^1 \mathbf{g}(\alpha) d\alpha &= \frac{1}{N} (H(\mathbf{X}|\mathbf{Y}(1)) - H(\mathbf{X}|\mathbf{Y}(0))) \\ &= \mathbf{R}(\lambda, \rho). \end{aligned} \quad (5)$$

It is convenient to assume that symbol k is transmitted through a channel with parameter α_k , and that each α_k is further characterized by a common parameter α in a smooth

and differentiable manner. For the case under consideration, we simply have $\alpha_k = \alpha$. Then define the k -th GEXIT function

$$g_k(\alpha_1, \dots, \alpha_{N/M}) = \frac{\partial H(\mathbf{X}|\mathbf{Y}(\alpha_1, \dots, \alpha_{N/M}))}{\partial \alpha_k}.$$

So, the GEXIT function is given by

$$g(\alpha) = \frac{1}{N} \sum_{k=1}^{N/M} g_k(\alpha_1, \dots, \alpha_{N/M}) \frac{\partial \alpha_k}{\partial \alpha}.$$

Lemma 1: Consider transmission using an LDPC code from the ensemble LDPC(N, λ, ρ) over the BICM channel with parameter α . Define $\phi_k(\mathbf{y}_{\sim k}) = \{p_{X_k|\mathbf{Y}_{\sim k}}(x|\mathbf{y}_{\sim k}), x \in \mathcal{X}\}$ and let $\Phi_k(\mathbf{Y}_{\sim k})$ be the corresponding random variable. Then, the k -th GEXIT function is given by

$$g_k(\alpha) = G(x_k(\mathbf{u}); \alpha) \triangleq \sum_{x_k \in \mathcal{X}} p(x_k) \int_{\mathbf{u}} x_{x_k}(\mathbf{u}) \kappa_{x_k}(\mathbf{u}) d\mathbf{u}, \quad (6)$$

where $x_k(\mathbf{u}) = \{x_{x_k}(\mathbf{u}), x_k \in \mathcal{X}\}$, and $x_{x_k}(\mathbf{u}) = p(\phi_k|x_k)$ is the distribution of ϕ_k assuming that $X_k = x_k$ was transmitted, and the GEXIT kernel is given by

$$\kappa_{x_k}(\mathbf{u}) = \int_y \frac{\partial}{\partial \alpha} p(y|x) \log_2 \frac{\sum_{x' \in \mathcal{X}} \mathbf{u}[x'] p(y|x')}{\mathbf{u}[x] p(y|x)} dy, \quad (7)$$

where $\mathbf{u}[j]$ denotes the j -th component of \mathbf{u} .

Proof: It can be verified that Φ_k is the extrinsic MAP estimator of X_k . We have

$$g_k(\alpha) = \frac{\partial H(\mathbf{X}|\mathbf{Y}(\alpha_1, \dots, \alpha_n))}{\partial \alpha_k} = \frac{\partial H(X_k|Y_k, \Phi_k)}{\partial \alpha_k}.$$

For notational convenience, we omit the dependence of X_k , Y_k and Φ_k on the symbol index k whenever possible. The conditional entropy of X_k is given by

$$\begin{aligned} H(X|Y, \Phi) &= - \int_{y, \phi} \sum_{x \in \mathcal{X}} p(x, y, \phi) \log_2 \frac{p(x, y, \phi)}{\sum_{x' \in \mathcal{X}} p(x', y, \phi)} dy d\phi \\ &= \sum_{x \in \mathcal{X}} p(x) \int_{\phi} p(\phi|x) \left(\int_y p(y|x) \log_2 \frac{\sum_{x' \in \mathcal{X}} p(x'|\phi) p(y|x')}{p(x|\phi) p(y|x)} dy \right) d\phi. \end{aligned}$$

This follows by noting that $p(x_k, y_k, \phi_k) = p(y_k|x_k) p(\phi_k|x_k) p(x_k)$. The result now follows by noting that $p(x_k|\phi_k) = p(x_k|\mathbf{y}_{\sim k})$.

Assuming that each bit in the symbol x_k is independent (which is true asymptotically as $N \rightarrow \infty$), we have

$$\begin{aligned} \mathbf{u} &= \left\{ \prod_{m=1}^M p(x_k^{[m]}|\mathbf{y}_{\sim k}), x_k \in \mathcal{X} \right\} \\ &\triangleq \{f_{x_k}(v_1, \dots, v_M), x_k \in \mathcal{X}\}, \end{aligned} \quad (8)$$

where $v_m = \log \frac{p(x_k^{[m]}=+1|\mathbf{y}_{\sim k})}{p(x_k^{[m]}=-1|\mathbf{y}_{\sim k})}$. From (8), we see that \mathbf{u} is completely characterized by v_1, \dots, v_M . So, (7) is henceforth interpreted in terms of the log-likelihood ratios v_m . ■

The density $x_k(\mathbf{u})$ in (6) is hard to compute, so instead one can use the BP estimate to compute the density for the asymptotic limit $N \rightarrow \infty$. The curve obtained by using the BP estimate is called the BP-GEXIT function $g^{\text{BP}}(\alpha)$. Let $\mathbf{x}^{(\ell)}(v)$

denote the density of the log-likelihood ratio, conditioned on the transmission of the all-zero codeword, emitted from the variable nodes to the detector nodes, during iteration ℓ . For a fixed ℓ , as the blocklength $N \rightarrow \infty$, we have $p_x(v_m) = \mathbf{x}^{(\ell)}(x^{[m]}v_m)$. If $F[x]$ is the density transformation operator corresponding to the map $\mu \mapsto e^\mu/(1+e^\mu)$, then we can write

$$\begin{aligned} \mathbf{x}(\mathbf{u}) &= \{p(\mathbf{u}|x), x \in \mathcal{X}\} \\ &= \left\{ \prod_{m=1}^M F[x](x^{[m]}v_m), x \in \mathcal{X} \right\}, \end{aligned} \quad (9)$$

where \mathbf{u} is given by (8). The BP-GEXIT function g^{BP} is computed as follows: For a given channel parameter α , compute the fixed point of density evolution, say \mathbf{a} . Then,

$$g^{\text{BP}}(\alpha) = G(F[L(\rho(\mathbf{a}))]; \alpha).$$

One can now calculate an upper bound on the MAP decoding threshold. The following procedure is now fairly standard and the details can be found in [14, Sec. 4.12]. It can be shown that the GEXIT functional G preserves degradation. So, by the optimality of the MAP decoder, the GEXIT function always lies below the BP-GEXIT function i.e., $g(\alpha) \leq g^{\text{BP}}(\alpha)$. Let $\bar{\alpha}$ be the largest positive number such that

$$\int_{\bar{\alpha}}^1 g^{\text{BP}}(\alpha) d\alpha = R(\lambda, \rho).$$

From the properties of the BP-GEXIT function and the GEXIT function, we have $\alpha^{\text{MAP}} \leq \bar{\alpha}$. Following [7], we refer to $\bar{\alpha}$ as the area threshold.

In this work we compute the BP-GEXIT curves for the case when there is no demapper update between iterations. The BP-GEXIT functions and the area threshold, for different BICM schemes are shown in Figures 4, 5, 6. The parameter α was chosen to be the normalized channel entropy per bit.

IV. SPATIALLY-COUPLED LDPC CODES

In this section, we describe the spatially-coupled $(1, r, L, w)$ ensemble introduced in [1]. The variable nodes are placed at positions $[-L, L]$ and the check nodes are placed at positions $[-L, L + w - 1]$ (w can be thought of as a ‘‘smoothing’’ parameter). Each of the 1 connections, of a variable node at position i , are uniformly and independently chosen from $[i, i + w - 1]$ as shown in Fig. 3. There are two consequences of this coupling - threshold increase and rate loss [1]. The design rate of a spatially-coupled $(1, r, L, w)$ ensemble is given by

$$R(1, r, L, w) = \left(1 - \frac{1}{r}\right) - \frac{1}{r} \frac{w + 1 - 2 \sum_{i=0}^w \left(\frac{i}{w}\right)^r}{2L + 1}.$$

Let $\mathbf{a}_i^{(\ell)}$ be the average density, in the spirit of (3), emitted by the variable nodes at position i . Set $\mathbf{a}_i^{(\ell)} = \Delta_{+\infty}$, the Dirac delta function at infinity, for $i \notin [-L, L]$. The DE for this ensemble can be written as

$$\begin{aligned} \mathbf{a}_i^{(\ell+1)} &= \phi \left(L(x_i^{(\ell)}); \sigma \right) \otimes \lambda(x_i^{(\ell)}) \\ x_i^{(\ell)} &= \frac{1}{w} \sum_{j=0}^{w-1} \rho \left(\frac{1}{w} \sum_{k=0}^{w-1} \mathbf{a}_{i+j-k}^{(\ell)} \right). \end{aligned} \quad (10)$$

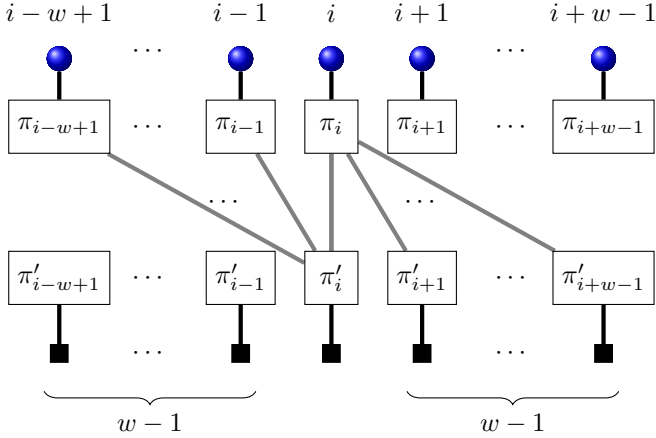


Fig. 3. A portion of a generic spatially-coupled code. The variable nodes are shown as blue filled circles and the check nodes are represented by black squares. The variable node at position i is connected to check nodes at positions $[i, i+w-1]$. The permutations π_i are chosen uniformly at random.

Here $L(x) = x^{\otimes 1}$, $\lambda(x) = x^{\otimes 1-1}$, and $\rho(x) = x^{\otimes r-1}$. For a channel parameter α , let $\bar{a} = [a_{-L}, \dots, a_L]$ denote the fixed point implied by (10). Using the technique developed in Section III, one can compute the GEXIT curves for spatially-coupled LDPC codes from (6) along the lines of [1]. Define the GEXIT functional for spatially-coupled codes via

$$G(\bar{a}) \triangleq \frac{1}{2L+1} \sum_{i=-L}^L G(a_i),$$

where $G(a)$ is defined in (6). The BP-GEXIT function of spatially-coupled codes is given in parametric form by $(\alpha, G(\bar{a}))$.

V. RESULTS

We consider the case when there is no demapper update between iterations. The BP-GEXIT curve of a $(3, 6, 64, 4)$ spatially-coupled ensemble is shown in Figures 4, 5, 6 for different BICM schemes. Figures 4, 5, 6 also demonstrate the threshold saturation phenomenon, wherein the BP threshold of the spatially-coupled ensemble is close to an intrinsic threshold of the underlying ensemble. For the optimal MAP demapper, this intrinsic threshold is the area threshold computed using the BP-GEXIT curve of the underlying ensemble. From Fig. 6, we observe that for the suboptimal MLM demapper, the BP threshold of the spatially-coupled code crosses the area threshold of the underlying ensemble.

It is known that increasing the left degree of regular LDPC codes, while keeping the rate constant, pushes the MAP threshold of the ensemble towards the noise threshold for BMS channels. Based on this, we compute the BP thresholds of a $(4, 8, 64, 4)$ and $(6, 12, 64, 4)$ spatially-coupled ensemble and as seen from Tables I and II, the gap to the BICM noise threshold indeed becomes smaller. The BP thresholds and the noise thresholds for the Rayleigh fast fading channel are shown in Tables I and II. The tables also show the asymptotic gap as the rate loss tends to zero, i.e., when $L \rightarrow \infty$. Based on this numerical evidence, we conjecture that the

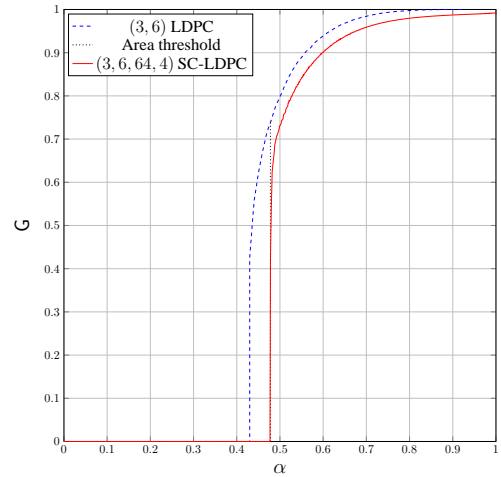


Fig. 4. The BP-GEXIT curve of a $(3, 6)$ code for QPSK modulation and the upper bound on the MAP threshold computed via the area theorem. Also shown is the BP-GEXIT curve of the $(3, 6, 32, 4)$ spatially-coupled ensemble.

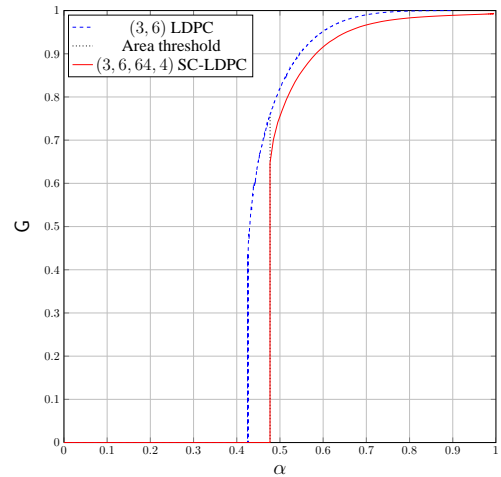


Fig. 5. The BP-GEXIT curve of a $(3, 6)$ code for 16QAM modulation with a MAP detector and the upper bound on the MAP threshold computed via the area theorem. Also shown is the BP-GEXIT curve of the $(3, 6, 32, 4)$ spatially-coupled ensemble.

ensemble of spatially-coupled LDPC codes with large left degrees universally approach the noise threshold for different BICM schemes.

The decoding thresholds of coding schemes for BICM can be improved by using BICM-ID. For comparison, the thresholds of the $(4, 8, 64, 4)$ spatially-coupled ensemble is computed for BICM-ID. The thresholds are computed for 64QAM modulation using a MAP demapper and we consider transmission over both AWGN and Rayleigh fast-fading channels. In this case, the demapper update was performed once for every 100 iterations of the spatially-coupled code. As expected, the gap to the noise threshold reduces to 0.09 dB from 0.20 dB and 0.24 dB for AWGN and Rayleigh fast-fading channels respectively. This improved performance comes at the expense of increased complexity.

TABLE I
PERFORMANCE OF VARIOUS SPATIALLY-COUPLED ENSEMBLES OVER BICM CHANNELS WITH A MAP DEMAPPER.

Mod. / Chan.	Noise Thresh. (E_b/N_0 in dB)	BP Thresh./Gap/Asympt. Gap (E_b/N_0 in dB)		
		(3, 6, 64, 4)	(4, 8, 64, 4)	(6, 12, 64, 4)
QPSK / AWGN	0.17	0.57/0.40/0.31	0.54/0.37/0.11	0.33/0.16/0.06
16QAM / AWGN	2.27	2.71/0.44/0.35	2.49/0.22/0.13	2.43/0.16/0.07
64QAM / AWGN	4.67	5.11/0.44/0.35	4.87/0.20/0.11	4.82/0.15/0.05
QPSK / Fading	1.83	2.27/0.44/0.35	2.04/0.21/0.12	2.00/0.17/0.07
16QAM / Fading	4.11	4.56/0.45/0.36	4.34/0.23/0.14	4.29/0.18/0.08
64QAM / Fading	6.62	7.11/0.49/0.40	6.86/0.24/0.15	6.80/0.18/0.08

TABLE II
PERFORMANCE OF VARIOUS SPATIALLY-COUPLED ENSEMBLES OVER BICM CHANNELS WITH AN MLM DEMAPPER.

Mod. / Chan.	Noise Thresh. (E_b/N_0 in dB)	BP Thresh./Gap/Asympt. Gap (E_b/N_0 in dB)		
		(3, 6, 64, 4)	(4, 8, 64, 4)	(6, 12, 64, 4)
QPSK / AWGN	0.17	0.57/0.40/0.31	0.54/0.37/0.11	0.33/0.16/0.06
16QAM / AWGN	2.29	2.70/0.41/0.32	2.51/0.22/0.13	2.47/0.18/0.08
64QAM / AWGN	4.71	5.14/0.43/0.34	5.00/0.29/0.20	4.96/0.25/0.15
QPSK / Fading	1.83	2.27/0.44/0.35	2.04/0.21/0.12	2.00/0.17/0.07
16QAM / Fading	4.17	4.63/0.46/0.37	4.41/0.24/0.15	4.36/0.19/0.09
64QAM / Fading	6.73	7.26/0.53/0.44	7.01/0.28/0.19	6.95/0.22/0.12

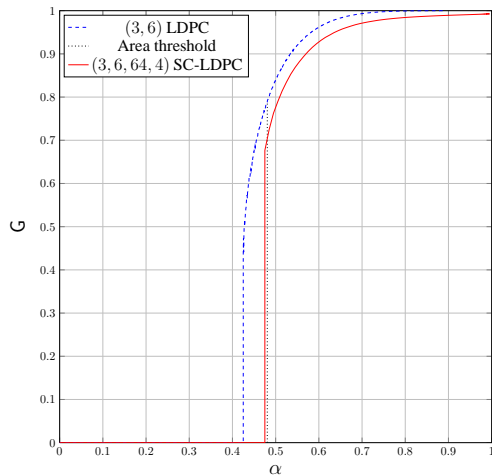


Fig. 6. The BP-GEXIT curve of a (3, 6) code for 16QAM modulation with an MLM detector and the upper bound on the MAP threshold computed via the area theorem. Also shown is the BP-GEXIT curve of the (3, 6, 32, 4) spatially-coupled ensemble.

VI. CONCLUDING REMARKS

Spatially-coupled LDPC codes have shown promising results for a large class of graphical models. In this work, we study their performance on BICM channels and validate the conjecture that the phenomenon of threshold saturation is indeed very general. We extend the GEXIT analysis of LDPC codes for BICM schemes. This enables one to bound the performance of the MAP decoder of LDPC codes. The area threshold, which upper-bounds the MAP decoding performance, of LDPC codes is computed for different demappers and modulations. Using these tools, we numerically demonstrate the phenomenon of threshold saturation for these channels. We note that when using suboptimal demappers (like the MLM demapper), the threshold saturates towards an intrinsic threshold of the suboptimal demapper and the upper bound computed using GEXIT curves is no longer tight. This is con-

sistent with previous results for spatially-coupled systems with suboptimal component decoders [20]–[22]. The performance also improves significantly when used with BICM-ID and the thresholds of SC-LDPC codes approach the noise threshold with smaller degrees. These asymptotic results demonstrate that SC-LDPC codes approach the noise threshold of different BICM schemes.

Irregular LDPC codes and multi-edge type LDPC codes were designed for BICM schemes in [18], [23] with excellent thresholds. In [19], the authors design families of protograph-based LDPC codes for BICM schemes with excellent thresholds of around 0.2-0.4 dB from the BICM noise threshold. For finite L , spatially-coupled codes compare favorably with the previously optimized LDPC ensembles in spite of the rate loss incurred due to finite L .

REFERENCES

- [1] S. Kudekar, T. J. Richardson, and R. L. Urbanke, "Threshold saturation via spatial coupling: Why convolutional LDPC ensembles perform so well over the BEC," *IEEE Trans. Inform. Theory*, vol. 57, no. 2, pp. 803–834, 2011.
- [2] J. Felstrom and K. S. Zigangirov, "Time-varying periodic convolutional codes with low-density parity-check matrix," *IEEE Trans. Inform. Theory*, vol. 45, no. 6, pp. 2181–2191, 1999.
- [3] M. Lentmaier, A. Sridharan, K. S. Zigangirov, and D. J. Costello, "Terminated LDPC convolutional codes with thresholds close to capacity," in *Proc. IEEE Int. Symp. Inform. Theory*, Adelaide, Australia, 2005, pp. 1372–1376.
- [4] M. Lentmaier and G. P. Fettweis, "On the thresholds of generalized LDPC convolutional codes based on protographs," in *Proc. IEEE Int. Symp. Inform. Theory*, Austin, TX, 2010, pp. 709–713.
- [5] M. Lentmaier, A. Sridharan, D. J. Costello, and K. S. Zigangirov, "Iterative decoding threshold analysis for LDPC convolutional codes," *IEEE Trans. Inform. Theory*, vol. 56, no. 10, pp. 5274–5289, Oct. 2010.
- [6] S. Kudekar, C. Méasson, T. Richardson, and R. Urbanke, "Threshold saturation on BMS channels via spatial coupling," in *Proc. Int. Symp. on Turbo Codes & Iterative Inform. Proc.*, Sept. 2010, pp. 309–313.
- [7] S. Kudekar, T. Richardson, and R. Urbanke, "Spatially coupled ensembles universally achieve capacity under belief propagation," in *Proc. IEEE Int. Symp. Inform. Theory*, July 2012, pp. 453–457.
- [8] S. Kumar, A. Young, N. Macris, and H. D. Pfister, "A proof of threshold saturation for spatially-coupled LDPC codes on BMS channels," in *Proc. 50th Annual Allerton Conf. on Commun., Control, and Comp.*, Oct. 2012.

- [9] T. T. Nguyen and L. Lampe, "Bit-interleaved coded modulation with mismatched decoding metrics," *IEEE Trans. Commun.*, vol. 59, no. 2, pp. 437–447, Feb. 2011.
- [10] A. Guillén i Fàbregas, A. Martinez, and G. Caire, *Bit-Interleaved Coded Modulation*. Now Publishers Inc., 2008, vol. 5, no. 1-2.
- [11] A. Alvarado, L. Szczecinski, R. Feick, and L. Ahumada, "Distribution of L-values in gray-mapped M^2 -QAM: closed-form approximations and applications," *IEEE Trans. Commun.*, vol. 57, no. 7, pp. 2071–2079, July 2009.
- [12] E. Zehavi, "8-PSK trellis codes for a Rayleigh channel," *IEEE Trans. Commun.*, vol. 40, no. 5, pp. 873–884, 1992.
- [13] J. Hou, P. H. Siegel, and L. B. Milstein, "Performance analysis and code optimization of low density parity-check codes on Rayleigh fading channels," *IEEE J. Select. Areas Commun.*, vol. 19, no. 5, pp. 924–934, May 2001.
- [14] T. J. Richardson and R. L. Urbanke, *Modern Coding Theory*. Cambridge University Press, 2008.
- [15] G. Caire, G. Taricco, and E. Biglieri, "Bit-interleaved coded modulation," *IEEE Trans. Inform. Theory*, vol. 44, no. 3, pp. 927–946, May 1998.
- [16] A. Martinez, A. Guillén i Fàbregas, G. Caire, and F. Willems, "Bit-interleaved coded modulation revisited: A mismatched decoding perspective," *IEEE Trans. Inform. Theory*, vol. 55, no. 6, pp. 2756–2765, June 2009.
- [17] J. Jaldén, P. Fertl, and G. Matz, "On the generalized mutual information of BICM systems with approximate demodulation," in *Proc. IEEE Inform. Theory Workshop*, Jan. 2010, pp. 1–5.
- [18] J. Hou, P. H. Siegel, L. B. Milstein, and H. D. Pfister, "Capacity-approaching bandwidth-efficient coded modulation schemes based on low-density parity-check codes," *IEEE Trans. Inform. Theory*, vol. 49, no. 9, pp. 2141–2155, Sept. 2003.
- [19] T. V. Nguyen, A. Nosratinia, and D. Divsalar, "Threshold of protograph-based LDPC coded BICM for Rayleigh fading," in *Proc. IEEE Global Telecom. Conf.*, Dec. 2011, pp. 1–5.
- [20] K. Takeuchi, T. Tanaka, and T. Kawabata, "Improvement of BP-based CDMA multiuser detection by spatial coupling," in *Proc. IEEE Int. Symp. Inform. Theory*, St. Petersburg, Russia, July 2011, pp. 1489–1493.
- [21] C. Schlegel and D. Truhachev, "Multiple access demodulation in the lifted signal graph with spatial coupling," in *Proc. IEEE Int. Symp. Inform. Theory*, St. Petersburg, Russia, July 2011, pp. 2989–2993.
- [22] Y.-Y. Jian, H. Pfister, and K. Narayanan, "Approaching capacity at high rates with iterative hard-decision decoding," in *Proc. IEEE Int. Symp. Inform. Theory*, July 2012, pp. 2696–2700.
- [23] H. Sankar, N. Sindhushayana, and K. Narayanan, "Design of low-density parity-check (LDPC) codes for high order constellations," in *Proc. IEEE Global Telecom. Conf.*, vol. 5, Nov. 2004, pp. 3113–3117.